Magnetic and neutron scattering experiments on the antiferromagnetic layer-type compounds K2Mn1-xMxF4 (M=Fe, Co)

Bevaart, L.; Frikkee, E.

DOI
10.1103/PhysRevB.18.3376

Publication date
1978

Published in
Physical Review. B, Condensed Matter

Magnetic and neutron scattering experiments on the antiferromagnetic layer-type compounds $K_2Mn_{1-x}M_xF_4$ (M = Fe,Co)

L. Bevaart and E. Frikkee
Netherlands Energy Research Foundation ECN, Petten, The Netherlands

J. V. Lebesque
Natuurkundig Laboratorium, University of Amsterdam, Amsterdam, The Netherlands

L. J. de Jongh
Kamerlingh Onnes Laboratory, University of Leiden, Leiden, The Netherlands

(Received 22 February 1978)

Substitution of Mn^{2+} in K_2MnF_4 by Fe^{2+} results in a randomly mixed two-component system with competing spin anisotropies, namely the axial dipolar anisotropy of the Mn^{2+} and Fe^{2+} ions, and the planar crystal-field anisotropy of the Fe^{2+} ions. For increasing amounts of Fe^{2+} the net (axial) anisotropy will initially decrease until it reaches a minimum, whereafter the net (planar) anisotropy increases. Magnetic measurements on single crystals $K_2Mn_{1-x}Fe_xF_4$ with $x = 0$, 0.008, 0.022 show indeed a decrease of the value of the spin-flop field with increasing x, which is expected for decreasing axial anisotropy. Since in these quasi $d = 2$ systems the transitions to three-dimensional long-range order ($d = 3$ LRO) are induced by the anisotropy, one expects T_c to vary with x. From susceptibility data for $x = 0.008$, 0.019, 0.022, 0.028, 0.061, and 0.125, and from neutron-scattering studies of the $d = 3$ LRO in the samples with $x = 0.022$, 0.028, 0.061, and 0.125, we conclude that for $0.022 < x < 0.028$ the value of T_c reaches a minimum, and the spin direction changes from the c axis to directions in the a-b plane, i.e., within the magnetic layers. It is found that T_c in the doped samples is as sharp as in pure K_2MnF_4. Furthermore, for $x = 0.022$ and 0.028 a spin reorientation to an intermediate direction is found at a temperature $T_R \simeq 1/2\,T_c$. Information about $d = 2$ correlations has been obtained by studying the intensity of scattered neutrons along the line $[\bar{1}/2\ \bar{1}/2\zeta]$ in reciprocal space. These ridge intensities for the $x = 0.022$ and 0.028 samples remain constant for $T_R < T < T_c - \Delta$ ($\Delta \simeq 4$ K), whereas they gradually disappear for $T < T_R$. In the $x = 0.022$ sample this constant ridge intensity is due to long-range $< S_x\,S_x >$ and $< S_y\,S_y >$ correlations. Here x and y define the spin components in the magnetic layer. The $d = 2$ LRO in the $x = 0.028$ sample for $T_R < T < T_c - \Delta$ is due to $< S_z\,S_z >$, $< S_y\,S_y >$, and $< S_x\,S_x >$ correlations. The coexistence of $d = 3$ LRO and $d = 2$ LRO can be explained by a mismatch in the correlations along the c axis between Fe^{2+} spins and Mn^{2+} spins in adjacent layers. Since the dipolar anisotropy increases with decreasing temperature, all spins gradually turn to a common orientation for $T < T_R$. The mismatch mechanism is thereby removed and $d = 2$ LRO is transferred into $d = 3$ LRO. For the other samples no spin-reorientation is found, since the large majority of the spins are either parallel to [001] (for $x < 0.022$) or within the layers (for $x > 0.028$). The x-T phase diagram obtained from the values of T_c and T_R, and from other ordering characteristics, consists of two lines at which either the z or the xy components order. These two lines cross in a tetracritical point, and encompass an intermediate phase. The critical behavior of the sublattice magnetization appears to depend sensitively on x. The critical index β is found to display a maximum in the region close to the tetracritical point.

I. INTRODUCTION

In the last few years one has witnessed a renewed interest of both theoretical and experimental workers in the study of magnetic systems containing magnetic or nonmagnetic impurities.[1] Recently, the critical behavior of the randomly mixed system $Rb_2Mn_{0.5}Ni_{0.5}F_4$ has been studied by neutron scattering.[2,3] Also a number of inelastic neutron scattering studies on such systems have been performed, e.g., $Rb_2Mn_{0.5}Ni_{0.5}F_4$,[4] which show profound changes in the magnetic excitation spectra, and on $Rb_2Mn_{1-c}Mg_cF_4$,[5] which can be related to percolation problems.

In this work we present neutron scattering, susceptibility, and magnetization data on the system $K_2Mn_{1-x}Fe_xF_4$, with x varying between 0.008 and 0.125. From the pioneering studies of Breed[6,7] and of Birgeneau *et al.*[8] it is known that the class of layered compounds A_2MF_4 (A = Rb or K; M is a $3d$-metal ion) are extremely good approximations of two-dimensional ($d = 2$) magnetic systems. The amount of spin-space anisotropy depends on the particular $3d$-metal ion involved. Thus K_2CoF_4 (Refs. 9–11) and Rb_2CoF_4 (Refs. 9 and 11) (transition temperatures $T_c = 107$ and 101 K,[9] respectively) are good examples of the quadratic layer Ising antiferromagnet because of the large axial crystal-field anisotropy of the Co^{2+} ions. K_2MnF_4 ($T_c = 42.3$ K)[12] and Rb_2MnF_4 (T_c

$= 38.4$ K)[8] can be regarded as $d=2$ Heisenberg antiferromagnets with a small amount of spin anisotropy. This spin anisotropy is also axial but in this case it is mainly due to the dipolar interactions between the Mn^{2+} spins ($S=\frac{5}{2}$), which establish a preference for the moments to point along the c axis (perpendicular to the magnetic layers). In the Fe^{2+} compounds Rb_2FeF_4 ($T_c=56$ K)[8,13] and K_2FeF_4 ($T_c\simeq 60$ K),[14] on the other hand, the spin anisotropy is very strong, originating once more from crystal-field effects. In contrast to the case of Co^{2+} and Mn^{2+}, the spin anisotropy for Rb_2FeF_4 and K_2FeF_4 is planar, forcing the $S=2$ moments to orient parallel to the magnetic layers. The anisotropy within the layers itself is very much smaller,[15] and the Fe^{2+} compounds may therefore be regarded as examples of the $d=2$ XY system. For more detailed information about the interaction parameters for the various compounds we refer to Table I.

For $d=2$ magnetic systems the occurrence of long-range magnetic order at a nonzero T_c is impossible in the case of pure Heisenberg or XY interactions.[16] However, the $d=2$ Ising model has a nonzero T_c,[17] and in general the presence of a spin anisotropy of the Ising type will lead to a finite ordering temperature.[18-21] Such an anisotropy-induced T_c would thus decrease if the amount of spin anisotropy is reduced. For the Mn^{2+} compounds the occurrence of three-dimensional long-range order ($d=3$ LRO) is thought to be induced primarily by the dipolar anisotropy. Although the interlayer interactions are needed to establish $d=3$ order, they present a much smaller perturbation ($\simeq 10^2$–10^3 times) than the spin anisotropy. The interpretation is therefore that the long-range order within the layers ($d=2$ LRO) is produced by the spin anisotropy which enables the simultaneous establishment of $d=3$ LRO through the interlayer interactions.

In order to reduce the "average" spin anisotropy K_2MnF_4 was doped with small amounts of Fe^{2+} ions. Such a reduction would result from the competition between the strong planar anisotropy of the Fe^{2+} ions and the much weaker axial anisotropy of the Mn^{2+} ions. For our present purposes we can approximate the interactions in our systems by the spin Hamiltonian:

$$\mathcal{H} = -2J \sum_{\langle i,j \rangle} \vec{S}_i \cdot \vec{S}_j - D \sum_i S_{iz}^2 , \qquad (1)$$

where i and j are lattice sites occupied by a spin S, and D is an anisotropy parameter. For K_2FeF_4 and K_2MnF_4 we have $D_{Fe}<0$, $|D_{Fe}|\simeq 0.01\,|J_{Fe}|$, and $D_{Mn}>0$, $|D_{Mn}|\ll|J_{Mn}|$, respectively. The intuitive picture one forms is that of Fe^{2+} impurity moments pinned within the layers by the crystal field. The nearest neighboring Mn^{2+} spins will be pulled nearly within the same direction because of the relatively strong antiferromagnetic Fe^{2+}-Mn^{2+} interactions. At larger distances from the Fe^{2+} site, the direction of the Mn^{2+} spins will

TABLE I. Ordering characteristics for several layered compounds. ϕ is the angle between the c axis and the spin direction.

	T_c (K)	J/k_B (K)	$D/2z\lvert J\rvert$	T_R (K)	Spin direction	β
K_2CoF_4 [a]	107	−97	$\simeq +0.7$		[001]	0.12
$K_2Mn_{0.98}Co_{0.02}F_4$	44.0				[001]	0.17(2)
$K_2Mn_{0.995}Co_{0.005}F_4$			$+9.1\times10^{-3}$		[001]	
K_2MnF_4 [a]	42.3	−4.2	$+3.9\times10^{-3}$		[001]	0.16
$K_2Mn_{1-x}Fe_xF_4$						
$x=0.008$			$+2.7\times10^{-3}$			
$x=0.022$	40.20(15)		$+1.4\times10^{-3}$	16(2)	$T_R<T<T_c$: [001]	0.19(2)
					$T=4$ K: $\phi=35(5)°$	
$x=0.028$	36.91(5)			19(2)	$T_R<T<T_c$: [110], [$\bar{1}$10]	0.28(2)
					$T=4$ K: $\phi=60(3)°$	
$x=0.061$	42.30(5)				[110], [$\bar{1}$10]	0.26(2)
$x=0.125$	44.0(1)				[110], [$\bar{1}$10]	0.21(2)
$(CH_3NH_3)_2FeCl_4$ [b]	94.5		$\simeq -0.1$		[110], [$\bar{1}$10]	0.15
K_2FeF_4 [c]	60	−7.5	$\simeq -0.1$		[110], [$\bar{1}$10]	
Rb_2FeF_4 [a]	56.0	−6.5	$\simeq -0.1$		[110], [$\bar{1}$10]	

[a] Values obtained from Ref. 15. [b] See Ref. 27. [c] See Ref. 14.

gradually become parallel to the c axis. Thus, around each Fe^{2+} ion there will be formed a cluster of Mn^{2+} ions with their spins "polarized" by the Fe^{2+} spins. For small Fe concentrations the extent of these clusters will be determined by the ratio of the antiferromagnetic exchange $|J_{Fe\text{-}Mn}|$ to the difference $|D_{Fe}| - |D_{Mn}|$. Although on a microscopic basis the system will be of a highly disordered character, the experimental results presented below show that nevertheless it is possible to consider average quantities such as sublattice magnetization and spin anisotropy to describe the macroscopic properties. Furthermore, the ordering temperature T_c is found to remain sharply defined and to vary indeed with the Fe concentration x.

For K_2CoF_4 the anisotropy parameter D_{Co} is positive, and $|D_{Co}| \simeq |J_{Co}|$. Consequently, there will be no competition between the spin-anisotropy terms for the Co^{2+} and Mn^{2+} ions in $K_2Mn_{1-y}Co_yF_4$, and the strong axial crystal-field anisotropy of the Co^{2+} ions is expected to increase the transition temperature with respect to pure K_2MnF_4. Indeed we observe an increase in T_c from 42.3 K for $y=0$ to 44.0 K for $y=0.02$.

We note that parts of our results have been discussed previously in a number of brief notes.[22-24] In the present paper the interest is focused on the influence of the impurity concentration or the average spin anisotropy, on the magnetic-ordering phenomena in these pseudo $d=2$ Heisenberg systems. The outline of the present paper is as follows. In Sec. II, we discuss experimental and structural details. In Secs. III and IV the results of the susceptibility and magnetization measurements and of the neutron-scattering studies are presented, respectively. Section V is devoted to the interpretation of these data.

II. EXPERIMENTAL DETAILS

The samples have been prepared by Breed from a mixture of KHF_2, MnF_2, and FeF_2. KHF_2 was used to provide a HF atmosphere to prevent oxidation. After heating this mixture to about 900 °C in a platinum crucible and subsequently cooling down to 750 °C in about 120 h, the $K_2Mn_{1-x}Fe_xF_4$ crystals were formed in the lower part of the crucible.

The chemical analyses of the samples have been performed by complexometric titrations with photometric endpoint detection. The iron was complexed with ethylene diamine tetra acetic acid (EDTA) and back titrated at pH = 2 with bismuth as a titrant and pyridyl azo resorcinol (PAR) as an indicator. Both manganese and iron were complexed with diamino cyclohexane tetra acetic acid (DCTA) and their sum was back titrated at pH = 5 with Ce(III) as titrant and xylenol orange as an indicator. Such analyses were performed for two or three crystals from each melt, resulting in the following values for the Fe^{2+} concentration in the six investigated samples: 0.8 ± 0.2, 1.9 ± 0.1, 2.2 ± 0.1, 2.8 ± 0.1, 6.1 ± 0.1, and 12.5 ± 0.5 at. % Fe. These concentrations are roughly a factor of 2 lower than the FeF_2 concentrations in the starting mixtures. The neutron-diffraction experiments were carried out on four samples, namely, with $x=0.022$, 0.028, 0.061, and 0.125, which weighed 89.8, 112.5, 38.4, and 125.1 mg, respectively.

In Fig. 1 the crystallographic and magnetic structure of K_2MnF_4 and the $(\bar{1}10)$ reciprocal-lattice plane are shown. This magnetic structure and the tetragonal symmetry allow the formation of two nonequivalent domains, namely, domains 1 with spins at (0, 0, 0) and $(\frac{1}{2}, \frac{1}{2}, \frac{1}{2})$ parallel and domains 2, where the spins in the plane $z=\frac{1}{2}$ are reversed. The neutron data presented in Sec. IV have been fitted with a model involving two nonequivalent domains with collinear spins, aligned ferromagnetically in the (110) and $(\bar{1}10)$ planes, and tilted over an angle ϕ with the c axis. For $\phi = 0°$ this model gives the K_2MnF_4 magnetic structure, while for $\phi = 90°$ the structure of K_2FeF_4 is obtained.[7,8,25]

The temperature dependence of the susceptibilities of the $K_2Mn_{1-x}Fe_xF_4$ samples has been deduced from magnetization measurements in the field interval 1–13 kOe, using a pendulum magnetometer described elsewhere.[26] The differential susceptibility, $\chi = \partial M/\partial H$, in the limit of $H \to 0$ was obtained by extrapolating $\chi(H) = M/H$ to zero field. For each sample the magnetization was measured with the field along the [001] or the [110] directions as determined in the neutron-diffraction experiments. The latter direction was chosen in

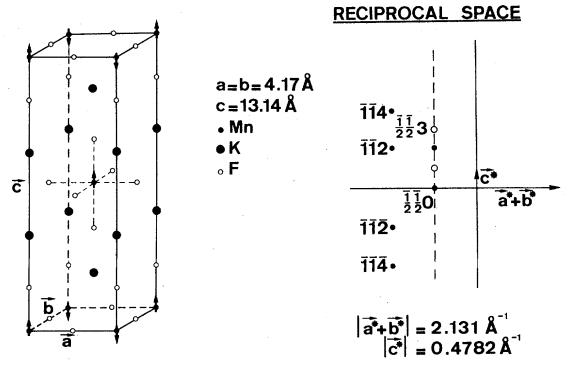

FIG. 1. Crystallographic unit cell and reciprocal lattice plane $(\bar{1}10)$ of K_2MnF_4. The indicated spin structure corresponds to domain-type 1 and superlattice reflections ○ in reciprocal space. The reflections ● are due to domain-type 2.

view of the magnetic structure for K_2FeF_4. Furthermore, for some Fe^{2+} concentrations the magnetization in high magnetic fields was measured in order to study the spin-flop phenomenon. These experiments were performed in the high-field setup in Amsterdam.[27]

The neutron scattering experiments were carried out on the HB3 spectrometer at the HFR reactor in Petten. In Fig. 2 the geometry of the apparatus is sketched. In front of the monochromator crystal a horizontal collimator of 20 min was used, while the vertical collimation in front of the sample due to the geometry was about 40 min. Behind the sample the horizontal as well as the vertical collimation amounted to 30 min. The wavelength of the neutrons was 1.475 Å, obtained from the (002) reflection of the Zn monochromator. The samples were glued onto an Al backing, with the [110] direction vertical and mounted in a He-flow cryostat. The temperature stability varied from 0.1% at $T \simeq 40$ K to 1% at $T \simeq 6$ K. A commercial, calibrated Ge resistor was used for the temperature detection. For each sample we have studied the superlattice reflections $(\frac{1}{2}\frac{1}{2}l)$, with $l = 0, 1, 2, 3$, which are directly related to the $d = 3$ LRO. The reflections $(\frac{1}{2}\frac{1}{2}l)$ with odd and even l correspond to domains 1 and 2, respectively. From these data we could determine the staggered magnetization as a function of temperature, the direction of the ordered spin components and the population of the domains. The $d = 2$ spin-spin correlations in the a-b plane are observed as lines of intensity in reciprocal space, parallel to the c^* axis [Fig 1(b)]. The ridge $[\frac{1}{2}\frac{1}{2}\zeta]$ has been investigated in the temperature range $4.4 \leq T \leq 60$ K at different positions ζ. From the ratios of the intensities for different ζ one may deduce which components of the spin system are contributing to the observed ridge intensities.

Besides the experiments on the $K_2Mn_{1-x}Fe_xF_4$ samples, a few measurements were performed on crystals of $K_2Mn_{1-y}Co_yF_4$. These Co^{2+} dopes were chosen in order to obtain an increase in the axial spin anisotropy with respect to the pure Mn compound. A few magnetic details will be reported. As regards neutron diffraction, measurements were performed on a sample which had $y = 0.02$ according to the analysis using the atomic-absorption method. The sample turned out to consist of a number of small crystallites, which prohibited a study of $d = 2$ scattering. The temperature dependence of $d = 3$ Bragg peaks of one of the crystallites could be followed, however.

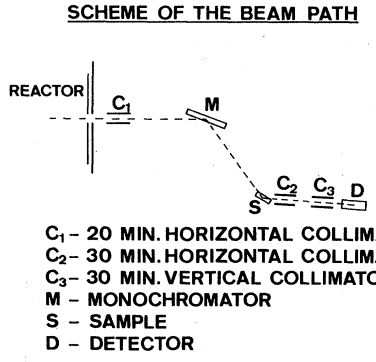

FIG. 2. Sketch of the neutron scattering experimental setup.

III. SUSCEPTIBILITY AND SPIN-FLOP MEASUREMENTS

In Figs. 3(a)–3(f) the susceptibilities $\chi(0)$ for $K_2Mn_{1-x}Fe_xF_4$ with varying x are shown as a function of temperature. Because there is no qualitative difference between the susceptibilities of the $x = 0.008$ and $x = 0.019$ samples, we do not present the data for $x = 0.019$ in this figure. For some samples we give the susceptibility $\chi(H)$ in the highest field applied ($H = 13$ kOe) as well as $\chi(0)$. The error bars denote the uncertainty in $\chi(0)$ introduced by the procedure of extrapolating $\chi(H)$ to zero field. In particular in the lower-temperature range, and for $x \geq 0.019$, these errors become substantial, as a consequence of the strong dependence of $\chi(H)$ upon the field (stronger than linear). All experimental susceptibilities have been corrected for a diamagnetic contribution of -0.79×10^{-4} emu/mole, as estimated from the known susceptibilities of KF, CaF_2, and ZnF_2. Corrections due to demagnetizing effects were negligibly small (<0.2%).

From Fig. 3 one may conclude that the behavior of χ in the paramagnetic region is hardly affected by the Fe^{2+} doping. In fact we find that within the experimental error of (1–2)% the data points for varying x all coincide with the curve for the pure K_2MnF_4 compound in the region $T \geq T_{max}$. Here T_{max} denotes the temperature at which the maximum in χ occurs. We find $T_{max} = 78 \pm 2$ K for all x, which is a strong indication that the "average" antiferromagnetic interaction remains practically the same. This may be understood from the following arguments: (i) the lattice constants of[12] K_2MnF_4 and[25] K_2FeF_4 are not much different ($a = 4.227$ and 4.14 Å, respectively); (ii) the spin values $S = 2$ and $S = \frac{5}{2}$ of Fe^{2+} and Mn^{2+} are nearly equal; (iii) the Fe^{2+}-Fe^{2+} intralayer superexchange constants $J/k_B = -6.5 \pm 1.5$ K estimated for Rb_2FeF_4,[15] and $J/k_B = -7.25 \pm 0.35$ K found in K_2FeF_4,[14] are not so much larger than that for Mn^{2+}-Mn^{2+} ($J/k_B = -4.20$ K)[6-8,15] and the Fe^{2+}-Mn^{2+} exchange will be between these values. Thus even with 10% of Fe^{2+} ions the changes in the "average" spin value and superexchange constant will be only about a few percent.

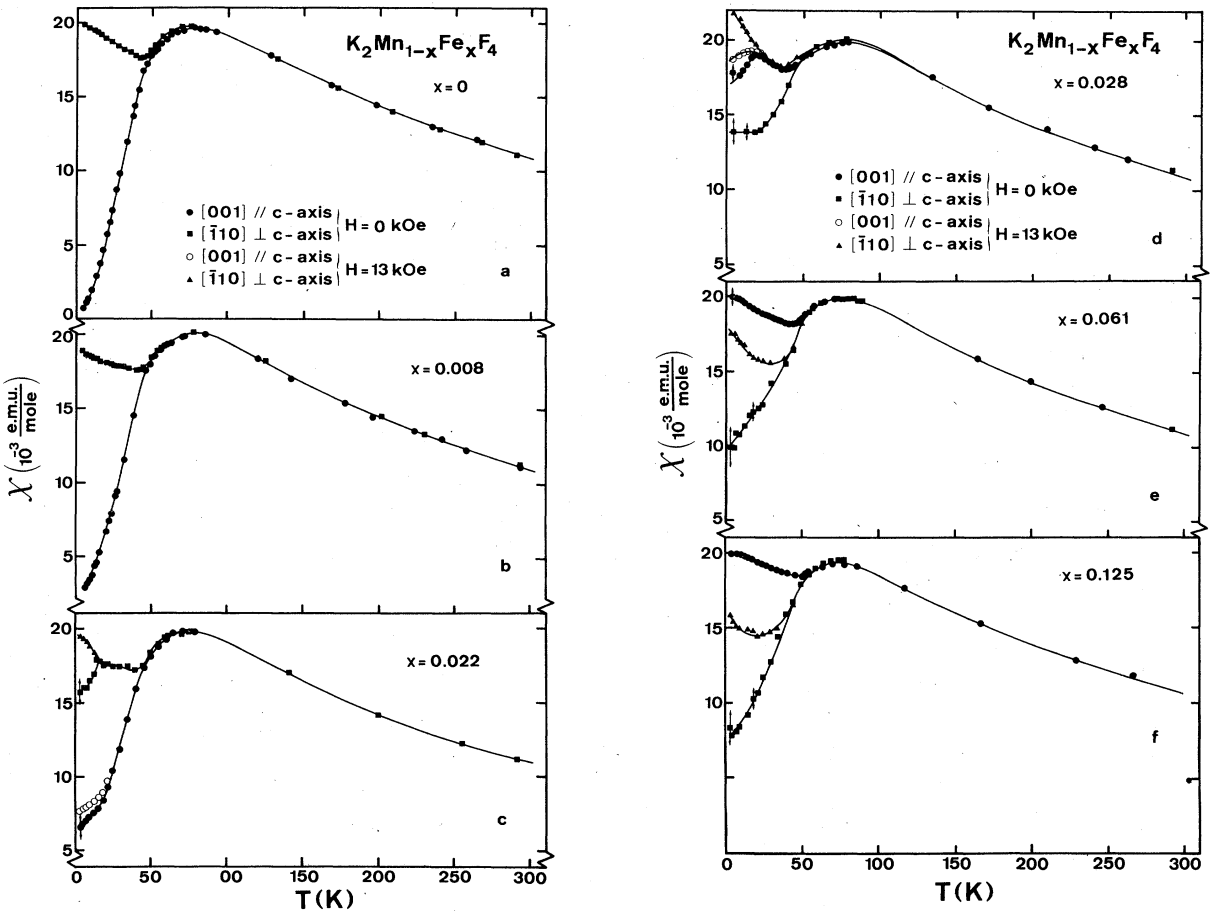

FIG. 3. Susceptibilities for the various $K_2Mn_{1-x}Fe_xF_4$ samples in $H=0$. For $x=0.022$, 0.028, 0.061, and 0.125 also the results in $H=13$ kOe are given for $T<T_{max}$. Here T_{max} is the temperature at which the susceptibility shows a maximum.

On the other hand, in the region of long-range magnetic ordering below $T\simeq 40$ K, the susceptibility behavior depends dramatically upon the Fe^{2+} concentration. For pure K_2MnF_4 the [001] direction clearly is also the axis of antiferromagnetic alignment. Along this direction the parallel susceptibility $\chi_{\parallel}$ is measured, which decreases to zero for $T\to 0$. Perpendicular to this axis the perpendicular susceptibility $\chi_{\perp}$ is measured, which depends only weakly on temperature. With increasing amount of Fe^{2+}, the value of $\chi_{[001]}(H=0)$ extrapolated to $T=0$ is seen to increase steadily, such that for $x\geq 0.028$ we even have $\chi_{[001]}(H=0) > \chi_{[110]}(H=0)$. This is a strong indication that for $x\leq 0.022$ the majority of the spins still have their direction parallel to the c axis, whereas for $x \geq 0.028$ the "average" direction of the moments is within the layers already.

We further note from Fig. 3 that for the $x=0.022$ and $x=0.028$ samples there is an abrupt change in χ at $T\simeq 16$ K and $T\simeq 20$ K, respectively. At these temperatures, which will be identified below with the spin reorientation temperatures T_R found in the neutron-diffraction study, discontinuities in the $\partial\chi_{[001]}/\partial T$ and $\partial\chi_{[110]}/\partial T$ are observed. The curves for $\chi(H=0)$ in this range are shown on an enlarged scale in Figs. 4(a) and 4(b).

The simplest model to explain these features is one in which the average spin orientation changes at T_R. For $x=0.022$ the change would be from a direction close to [001], to a direction tilted away from the c axis. For $x=0.028$ it would be from an orientation nearly within the layer to a direction closer to the c axis. The discussion of these phenomena will be taken up again in Sec. V, together with the neutron-diffraction data.

To further understand the extreme dependence on H in the region $T<T_R$ for $x=0.022$ and $T<T_c$ for $x\geq 0.028$ we note the following. As mentioned in Sec. II the moments in pure K_2FeF_4 are oriented either along the [110] or the [$\bar{1}$10] directions. Assuming that both the [110] and [$\bar{1}$10] domains will

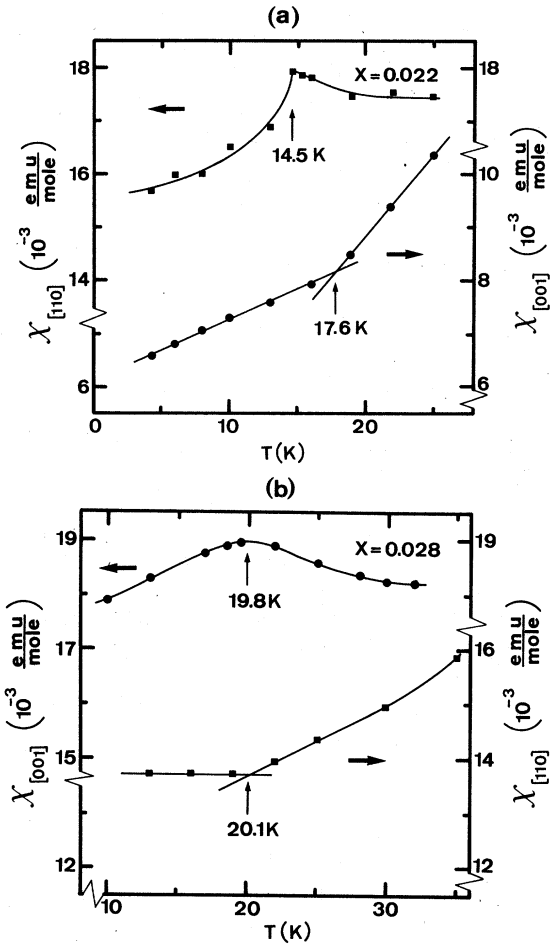

FIG. 4. (a) Susceptibilities $\chi[110]$ and $\chi[100]$ in $H=0$ for $x=0.22$ and for temperatures around T_R. (b) Same as in (a), but now for $x=0.028$.

be equally populated, the susceptibility $\chi_{[110]}(H=0)$ for K_2FeF_4 will be a mixture of the contributions of the two domains, so that we would have $\chi_{[110]} = \frac{1}{2}(\chi_{\parallel} + \chi_{\perp}^{in})$. Furthermore, we would have $\chi_{[001]} = \chi_{\perp}^{out}$. Here $\chi_{\parallel}$ denotes the susceptibility parallel to the Fe^{2+} spins in a single domain, whereas $\chi_{\perp}^{in}$ and $\chi_{\perp}^{out}$ denote the perpendicular susceptibilities within the layer, and perpendicular to the layer, respectively. For pure K_2FeF_4 the anisotropy within the layer is very much smaller than the out-of-plane anisotropy. For the Fe^{2+} impurities in $K_2Mn_{1-x}Fe_xF_4$ we similarly expect the spin direction to be either parallel to [110] or to $[\bar{1}10]$, with a small in-plane anisotropy. Accordingly, for $\vec{H} \parallel [110]$ or $[\bar{1}10]$ those Fe^{2+} moments which are initially parallel to the applied field will orient themselves perpendicular to the field direction for very small values of H already.

As regards the field dependence for $\vec{H} \parallel [001]$, we may understand this on basis of the delicate balance between the planar Fe^{2+} spin anisotropy and the axial Mn^{2+} dipolar spin anisotropy, as is evident, e.g., from the occurrence of the reorientation transitions. It follows that even small fields may tip the scales.

For the $x=0.061$ and $x=0.125$ samples the Fe^{2+} concentration is large enough to keep the moments within the layers at all temperatures. Even for the $x=0.061$ sample the "average" planar anisotropy is already quite substantial, since we find $\chi_{[001]}$ to be independent of field up to $H=13$ kOe. The H dependence for $\vec{H} \parallel [110]$ remains, and is of the same order for $x=0.061$ and $x=0.125$ as for $x=0.028$. This is to be expected since it is due to the just-described reorientation mechanism for the spins within the layers, in which only the small in-plane anisotropy is involved.

From the values of $\chi_{[001]}(H=0)$ and $\chi_{[110]}(H=0)$ extrapolated to zero temperature, we can obtain estimates for the average spin direction in the various samples, using a simple molecular-field model. If the spins make an angle ϕ with the c axis [001], and if the xy components of the spins are equally distributed among [110] and $[\bar{1}10]$, then we have for $H \to 0$ and for small spin anisotropies the following approximate formulas at $T=0$:

$$\chi_{[001]} = \chi_{\perp}^{MF} \sin^2\phi \,, \tag{2}$$

$$\chi_{[110]} = \tfrac{1}{2}\chi_{\perp}^{MF}(1+\cos^2\phi) \,. \tag{3}$$

In these expressions $\chi_{\perp}^{MF} = N_A g^2 \mu_B^2 / 4z|J|$, i.e., the perpendicular susceptibility of an antiferromagnet in the molecular-field approximation, where N_A is Avogadro's number, g the gyromagnetic ratio, μ_B the Bohr magneton, and z the number of nearest neighbors.

For the $x=0.022$ sample we have $\chi_{[001]}(H=0) = (6.2 \pm 0.2) \times 10^{-3}$ emu/mole and $\chi_{[110]}(H=0) = (15.5 \pm 1.0) \times 10^{-3}$ emu/mole for $T \to 0$. Using the value $J/k_B = -4.20$ K mentioned above we find $\phi = 37° \pm 2°$ from $\chi_{[001]}$ and $\phi = 46° \pm 8°$ from $\chi_{[110]}$. For the $x=0.028$ sample the corresponding values are $\chi_{[001]} = (16.9 \pm 0.5) \times 10^{-3}$ emu/mole, yielding $\phi = 71° \pm 5°$ and $\chi_{[110]} = (13.8 \pm 1.0) \times 10^{-3}$ emu/mole, leading to $\phi = 58° \pm 8°$. Summarizing, we would have $\phi \simeq 40°$ and $\phi \simeq 65°$ for $x=0.022$ and 0.028, respectively, according to the crude model used.

A determination of the ordering temperatures $T_c(x)$ from the measured susceptibility curves is not without ambiguity. Obviously, the onset of an anisotropy in χ is not a clear criterion. All samples show a marked anisotropy for $T \lesssim 40$ K, although above this temperature some differences between $\chi_{[001]}$ and $\chi_{[110]}$ can already be seen. Theoretically, the T_c of an antiferromagnet can be identified as the temperature at which the temperature derivative of the parallel susceptibility reaches a maximum. However, our χ data are

not detailed enough to obtain accurate determinations in this way. On the other hand, the temperatures at which the perpendicular susceptibility has a minimum are well defined. We find $T_{min}=43$, 41.5, 42, 38, 45, and 50 K for $x=0.008$, 0.019, 0.022, 0.028, 0.061, and 0.125, respectively. For pure K_2MnF_4 Breed has reported $T_{min}=45$ K.[6] We may compare these values with the T_c's derived from the neutron-diffraction data (cf. Table I). Although the agreement is not complete, both sets of data show the same trend.

Concluding this section we discuss the high-field magnetization measurements taken at 4.2 K with $\vec{H} \parallel [001]$ on the $x=0.008$ and $x=0.022$ samples, as shown in Fig. 5(a). For comparison we include in Fig. 5(b) results of Breed[6,7] on pure K_2MnF_4 and on a sample of K_2MnF_4 doped with 0.5% Co^{2+}. As expected, by the substitution of the Mn^{2+} ions by Co^{2+} or Fe^{2+} the value of the spin-flop field H_{SF} is increased or decreased, respectively. By H_{SF} we denote the field at which the moments turn to a direction perpendicular to the applied field because the anisotropy energy is overcome by the difference in magnetic field energy between the perpendicular and parallel orientations. The spin flop should show up as a discontinuous jump in the M-H curve. In practice this jump can be smeared out due to, e.g., inhomogeneities or small misorientations. For the K_2MnF_4 data of Breed in Fig. 5(b) the smearing is clearly due to the fact that the experiment was performed on a number of small single crystals, piled on top of one another to obtain enough sensitivity.[6,7] In case of the doped samples we may expect a distribution around the average value of the anisotropy since a Mn^{2+} ion will be subject to a different anisotropy field depending on its distance from a Fe^{2+} impurity.

For K_2MnF_4 and $K_2Mn_{0.995}Co_{0.005}F_4$ Breed[6,7] has derived the spin-flop fields as $H_{SF}=55.2\pm0.8$ and $H_{SF}\simeq 85$ kOe, respectively. From these results one obtains for the anisotropy parameter $|D/2zJ|$ the values $|D/2zJ|=3.9\times10^{-3}$ and 9.1×10^{-3} for K_2MnF_4 and $K_2Mn_{0.995}Co_{0.005}F_4$, respectively. For $K_2Mn_{0.992}Fe_{0.008}F_4$ and $K_2Mn_{0.978}Fe_{0.022}F_4$ we find similarly $H_{SF}\simeq 46$ and $\simeq 33$ kOe, leading to $|D/2zJ|=2.7\times10^{-3}$ and 1.4×10^{-3}, respectively. Below we will show that for the doped samples the transition temperature remains well defined, and that the value of $T_c(x)$ can be correlated with the anisotropy parameter D.

IV. NEUTRON-DIFFRACTION DATA

A. Three-dimensional ordering

The temperature dependences of the four reflections $(\frac{1}{2}\frac{1}{2}l)$ with $l=0$–3 are shown in Figs. 6 and 7 for the $x=0.022$ and $x=0.028$ samples, respectively. Discontinuities in $\partial I/\partial T$ are observed at temperatures T_R of about 16 and 19 K for $x=0.022$ and $x=0.028$. From the change in the relative intensities of magnetic reflections cor-

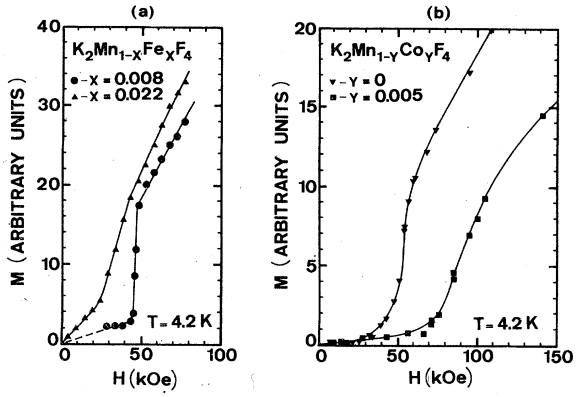

FIG. 5. (a) Spin-flop measurements for $x=0.008$ and 0.022. (b) Spin-flop measurements performed by Breed on K_2MnF_4 and $K_2Mn_{0.995}Co_{0.005}F_4$.

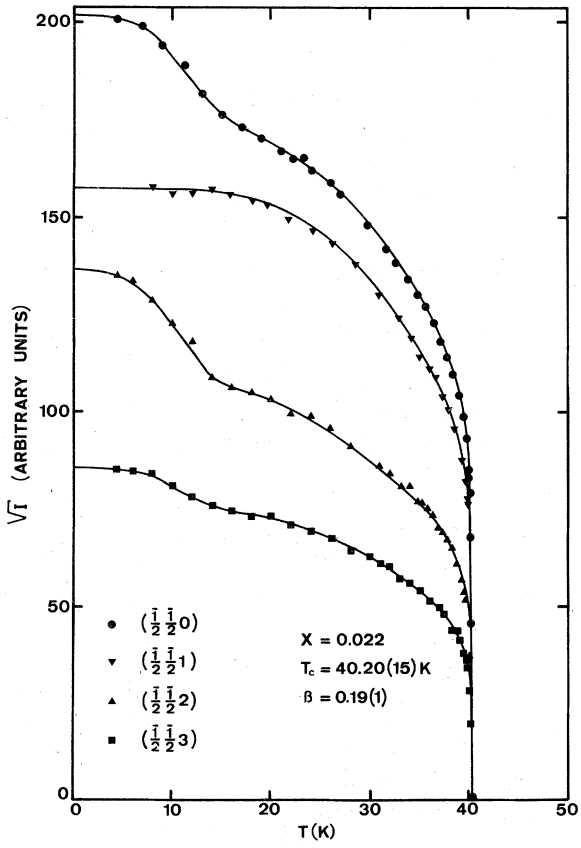

FIG. 6. Temperature dependence of the measured superlattice reflections in $K_2Mn_{0.978}Fe_{0.022}F_4$. $\sqrt{I}$ is the square root of the intensity. β denotes the critical index of the sublattice magnetization.

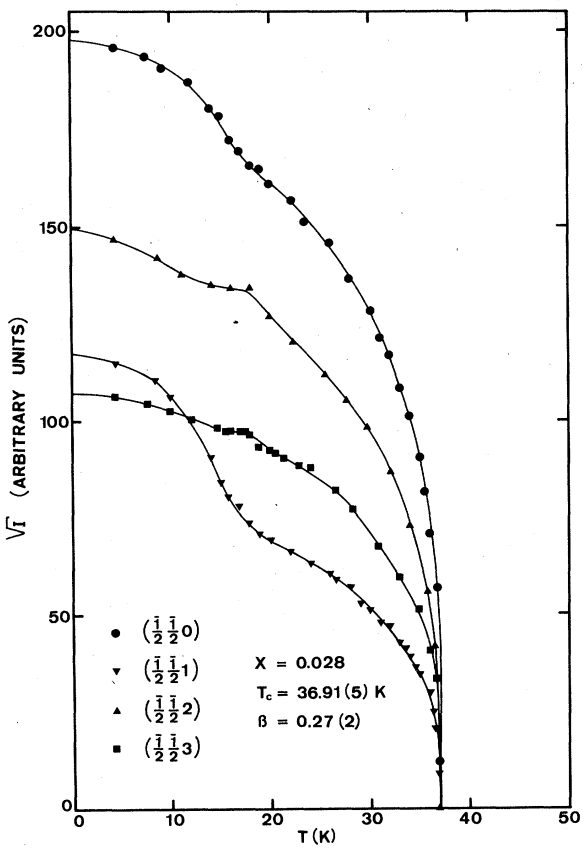

FIG. 7. Temperature dependence of the measured superlattice reflections for $K_2Mn_{0.972}Fe_{0.028}F_4$.

responding to the same domain type [e.g., the $(\bar{\frac{1}{2}}\bar{\frac{1}{2}}1)$ and $(\frac{1}{2}\frac{1}{2}3)$ reflections in Figs. 6 and 7] it may be concluded that a spin reorientation occurs for $T < T_R$. Also from the ratios of the intensities it is found that for $x = 0.022$ the moments are parallel to the c axis for $T_R < T < T_c$. Below T_R the moments rotate gradually away from the c axis, resulting in a mean angle $\phi = 35° \pm 5°$ with the c axis at $T = 4.4$ K. A similar reorientation is found for the $x = 0.028$ sample below 19 K. However, in that case the reorientation is in the reverse direction, since the moments turn from a direction within the layers for $T_R < T < T_c$ towards an angle $\phi = 60° \pm 3°$ at $T = 4.4$ K. The neutron-diffraction data thus confirm the mean directions of the sublattice magnetizations both for $T_R < T < T_c$ and at $T \simeq 0$ deduced in Sec. III from the χ measurements.

The reorientation process will be the result of the competition between the crystal field and the dipolar spin anisotropies. Of these the crystal-field anisotropy will be nearly independent of temperature, whereas the dipolar anisotropy will vary like some power of the average magnetization. Accordingly, the "net anisotropy" will vary with the temperature and may even change sign, which explains the spin reorientation. Furthermore, it will obviously not be homogeneous on a microscopic scale. This explains why the observed T_R's are not very sharp. The reorientation phenomenon is only observed for the above-mentioned two samples. From the χ data for the $x = 0.008$ and $x = 0.019$ samples (cf. Fig. 3) we conclude that in the ordered region the moments remain parallel to the c axis. For the $x = 0.061$ and $x = 0.125$ samples both the susceptibility and the neutron data show that for $T \leq T_c$ the moments are within the layers. In Table II the experimental and the calculated intensity ratios of the four measured reflections have been collected for the various investigated samples.

We mention that the more or less abrupt changes in the $d = 3$ scattering observed at T_R cannot be due to reorientation of the moments only. This follows for instance from the fact that the $(\bar{\frac{1}{2}}\bar{\frac{1}{2}}0)$ reflection should not be influenced by the reorientation, if the above mentioned model involving two nonequivalent domains with collinear spins, aligned ferromagnetically in the (110) and $(\bar{1}10)$ planes is correct. In Sec. IV B. we shall infer from the temperature dependences of the ridge intensities that the extra increases in the sublattice magnetization are due to a gradual transfer from $d = 2$ into $d = 3$ intensity below T_R.

Furthermore, the relative populations of the domains 1 and 2 as discussed in Sec. II, can be deduced from the intensities of the magnetic reflections. Within the experimental error of about 5% our results indicate a 50–50 distribution over the two domains for all the investigated samples.[22,23]

In contrast with the reorientation temperatures T_R the observed transition temperatures $T_c(x)$ are well defined and sharp, in spite of the microscopic inhomogeneities introduced by the Fe impurities. That is, within the errors the temperatures $T_c(x)$ appear to be as sharp as that found for pure K_2MnF_4. As an example we show in Fig. 8 the intensity of the $(\bar{\frac{1}{2}}\bar{\frac{1}{2}}0)$ reflection of the $x = 0.028$ sample near T_c. A small amount of critical scattering is observed, which is only ~1% of the $(\bar{\frac{1}{2}}\bar{\frac{1}{2}}0)$ intensity at $T = 4.4$ K. As will be shown it is mainly due to $d = 2$ scattering. Using the measured temperature dependence of the ridge intensity, this contribution can be easily subtracted from the peak intensities. Such corrections have been applied to all the data shown in this section.

The ordering parameters obtained for the various samples have been collected in Table I. It can be seen that the value of $T_c(x)$ passes through a minimum with increasing x. The initial decrease of $T_c(x)$ can be clearly related with the

TABLE II. Experimental and calculated intensities of the four measured reflections for the various investigated samples. The intensities are normalized with respect to the $(\frac{1}{2}\frac{1}{2}0)$ reflection. The angle ϕ between the c axis and the spin direction at $T=4.4$ K is obtained from the difference between the intensities of each individual reflection at $T=24$ K and $T=4.4$ K, assuming that the spins for $T=24$ K point along symmetry axes. For these calculations a model involving two nonequivalent domains is used.

	$\vec{S}\parallel[001]$ Calc.[a]	$x=0.022$ $T=24$ K	$x=0.022$ $T=4.4$ K	ϕ (deg)	ϕ (deg)	$x=0.028$ $T=4.4$ K	$x=0.028$ $T=24$ K	$x=0.061$	$x=0.125$	$\vec{S}\parallel[110]$ and $[\bar{1}10]$ Calc.
$(\frac{1}{2}\frac{1}{2}0)$	100	100	100			100	100	100	100	100
$(\frac{1}{2}\frac{1}{2}1)$	75.1	86.1±1.3	62.2±0.2	36± 2	59±2	37.3±0.6	17.8±0.4	14.8±0.4	14.9±0.4	14.8
$(\frac{1}{2}\frac{1}{2}2)$	38.2	36.7±0.7	45.5±0.8	33± 2	57±2	76.3±1.1	87.5±1.3	69.5±1.2	60.3±1.1	68.3
$(\frac{1}{2}\frac{1}{2}3)$	17.3	17.8±0.4	17.8±0.4	20±20	62±4	37.0±0.5	40.9±0.6	27.9±0.6	25.9±0.6	30.5

[a] See Ref. 8.

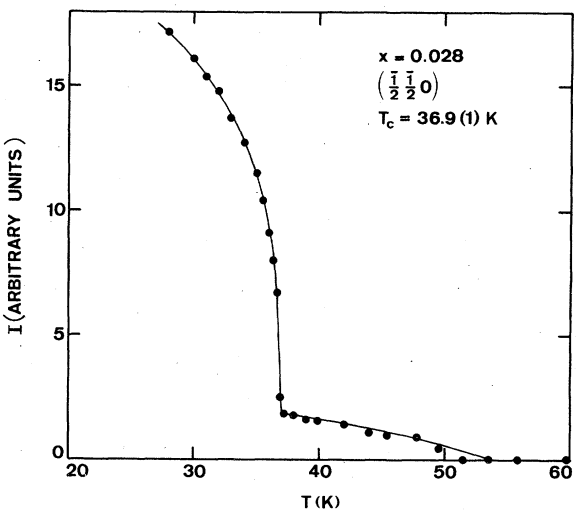

FIG. 8. Temperature dependence around T_c of the intensity I of the $(\frac{1}{2}\frac{1}{2}0)$ reflection for $x=0.028$.

decrease in the net axial anisotropy (see the values for $|D/2zJ|$ in Table I). For $x \geq 0.028$ the Fe concentration is apparently large enough for the net anisotropy to become planar. Upon increasing this planar anisotropy (by increasing x) the value of T_c is seen to rise again to that found for pure K_2FeF_4. The variation of T_c (and T_R) with x is shown in the phase diagram given in Fig. 9.

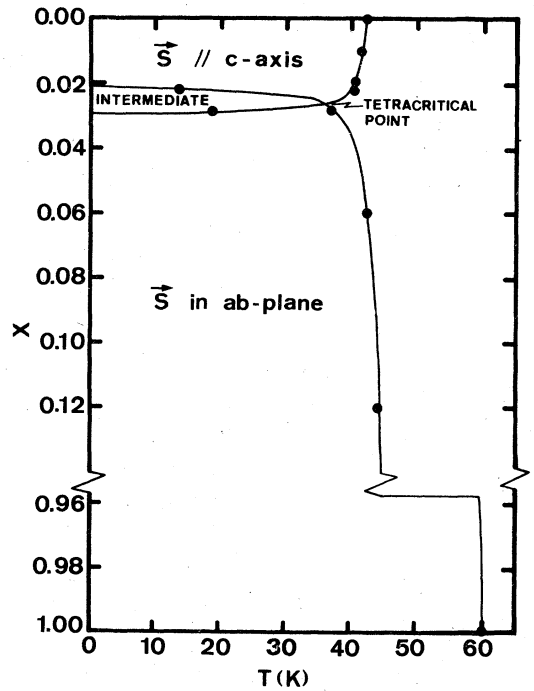

FIG. 9. x-T phase diagram for $K_2Mn_{1-x}Fe_xF_4$. The phase diagram contains two lines, at which either the z or the xy components order.

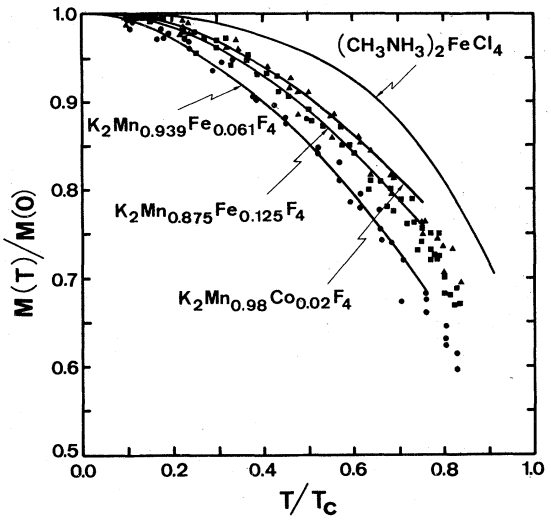

FIG. 10. Normalized sublattice magnetization vs the reduced temperature for several samples in a temperature range $T/T_c < 0.85$. The curve for K_2MnF_4 coincides with that for $K_2Mn_{0.875}Fe_{0.125}F_4$.

The parameters for the $K_2Mn_{0.98}Co_{0.02}F_4$ sample have been included in Table I. For this sample only the Bragg reflections $(\frac{1}{2}\frac{1}{2}l)$ were followed as a function of temperature. As expected from the larger axial anisotropy the value of T_c exceeds that of the pure K_2MnF_4 compound. The spin direction is parallel to the c axis in the whole region below T_c.

For the $K_2Mn_{0.98}Co_{0.02}F_4$ sample and for the $x = 0.061$ and $x = 0.125$ samples, the reflections with different l can be scaled upon one another in each case. In Fig. 10 the temperature dependences of the normalized sublattice magnetizations obtained in this way are compared with the results for pure K_2MnF_4,[28] and for $(CH_3NH_3)_2FeCl_4$ (a magnetic system equivalent to K_2FeF_4).[29]

It is found that outside the critical region the curve for the Co-doped sample lies above the K_2MnF_4 curve, whereas the doping with 6.1 at. % Fe^{2+} results in a decrease of the sublattice magnetization with respect to the pure Mn^{2+} compound. On the other hand, the curve for $x = 0.125$ coincides with that of K_2MnF_4, and for $(CH_3NH_3)_2FeCl_4$ the magnetization curve is above the K_2MnF_4 result.

The differences in behavior for the various samples in Fig. 10 will have to be explained on basis of a variation in the ratio of in-plane to out-of-plane spin anisotropies. For pure K_2MnF_4 the in-plane anisotropy is zero, the only term being the axial out-of-plane anisotropy. At the other extreme the compound $(CH_3NH_3)_2FeCl_4$ will have a weak in-plane anisotropy as compared to the strong planar anisotropy establishing the easy plane of magnetization. Since both the $d = 2$ Heisenberg and planar (XY) models cannot sustain long-range order, the planar anisotropy itself does not lead to an ordered state, and an in-plane anisotropy component is needed to produce a nonzero sublattice magnetization at any finite temperature. For the planar systems the in-plane anisotropy thus plays the same role as the axial anisotropy in a Heisenberg system. The sensitivity of the magnetization to the ratio of both types of anisotropy is therefore to be expected. Spin-wave theoretical calculations of the sublattice magnetizations, in which both the in-plane and the out-of-plane anisotropies are taken into account, are in progress.[30]

The sublattice magnetization $M_s(T)$ in the critical region is generally accepted to be described by the power law $M_s(T) \sim \epsilon^\beta$. Here ϵ is the relative temperature $1 - T/T_c$, and β is the critical index for the magnetization. For $d = 3$ lattices the values $\beta = 0.31$ and $\beta = 0.36$ have been deduced in case of Ising or Heisenberg interactions, respectively.[31] For $d = 2$ lattices only the Ising model can show a long-range order, and the value of $\beta = \frac{1}{8}$ appears to be an exact result.[17] In the case of an anisotropy-induced phase transition in a nearly isotropic $d = 2$ lattice one would expect the same Ising value for β to apply on basis of universality arguments. This has indeed been confirmed experimentally.[8,10,11] We further remark that the extent of the critical region for the magnetization will in general be limited to $\epsilon \leq 5 \times 10^{-2}$.[32]

The log-log plots for the sublattice magnetizations of our doped samples are compared in Fig. 11. In this figure the results from the $(\frac{1}{2}\frac{1}{2}0)$ reflections for the various samples are shown. A common feature of these plots is the fact that the power-law behavior appears to extend to very high values of ϵ, namely, to $\epsilon \simeq 0.5$ or even higher. This has also been observed in the pure compounds K_2MnF_4, Rb_2MnF_4, and K_2NiF_4. The reason is probably not that for these systems indeed the critical region extends to such a high ϵ value, but that by coincidence the magnetization behavior in the spin-wave region of these quasi-Heisenberg compounds joins smoothly into the critical behavior.[33]

Be this as it may, we may deduce apparent values for β from the plots in Fig. 11, and these values depend rather strongly upon the impurity concentration. In order to demonstrate that the value of β is the same for each of the reflections for a particular sample, the data for the $(\frac{1}{2}\frac{1}{2}l)$ reflections of the $x = 0.028$ sample with $l = 1, 2, 3$ are shown in Fig. 12. A comparison with the $(\frac{1}{2}\frac{1}{2}0)$ reflection in Fig. 11 shows that the slopes for $T > T_R$ are the same, although the behavior for $T < T_R$ is different (see also Fig. 7).

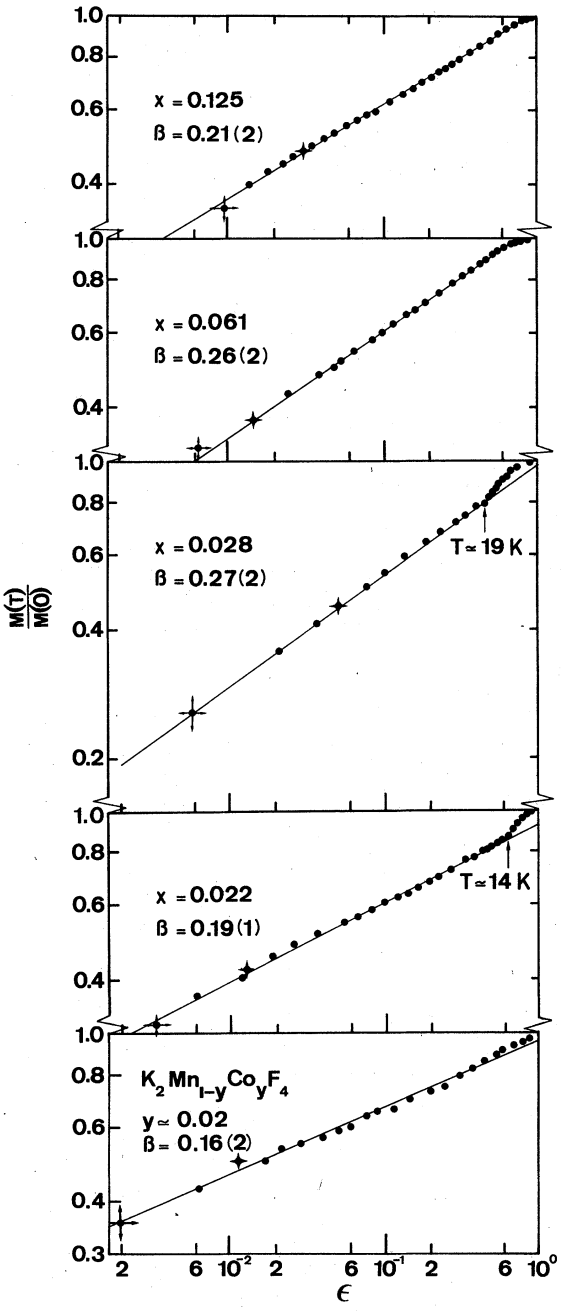

FIG. 11. Normalized sublattice magnetization vs $\epsilon \equiv 1 - T/T_c$, on a double logarithmic scale, for the samples investigated by neutron scattering. Data points refer to the $(\frac{1}{2}\frac{1}{2}0)$ reflections.

B. Two-dimensional correlations and long-range order

The study of the $d=2$ ridge intensity yields some interesting new phenomena for the two samples which show the reorientation effect. For these two samples the temperature dependences of the measured ridge intensities, obtained from scans perpendicular to the ridge, are shown in Figs. 13

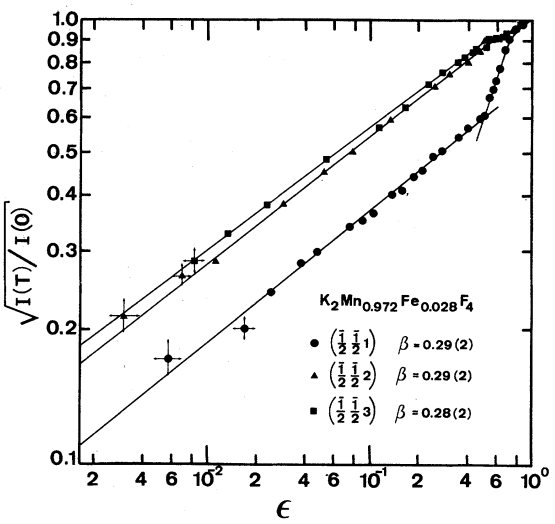

FIG. 12. Square root of the normalized intensity vs ϵ for the reflections $(\frac{1}{2}\frac{1}{2}l)$ with $l=1$, 2, 3 and for the $x=0.028$ sample.

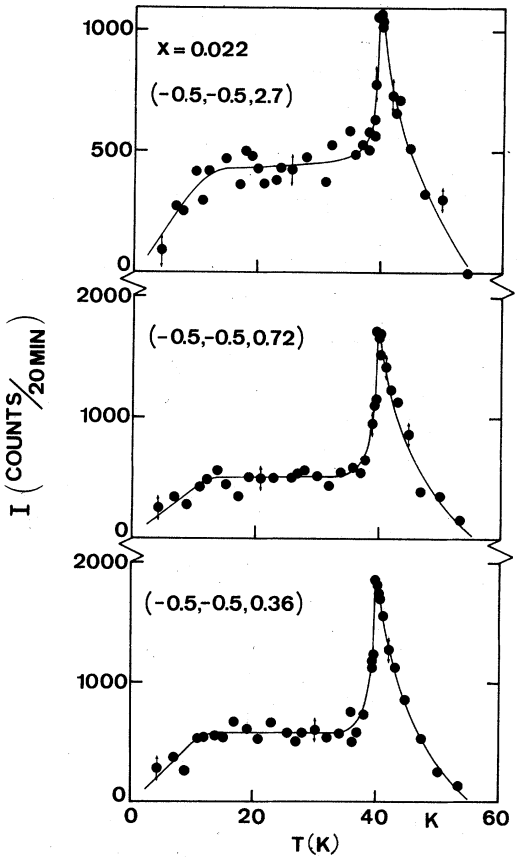

FIG. 13. Temperature dependences of the intensity of the ridge $[\frac{1}{2}\frac{1}{2}\zeta]$ for $x=0.022$ and for several ζ. Note the different scale in the upper plot.

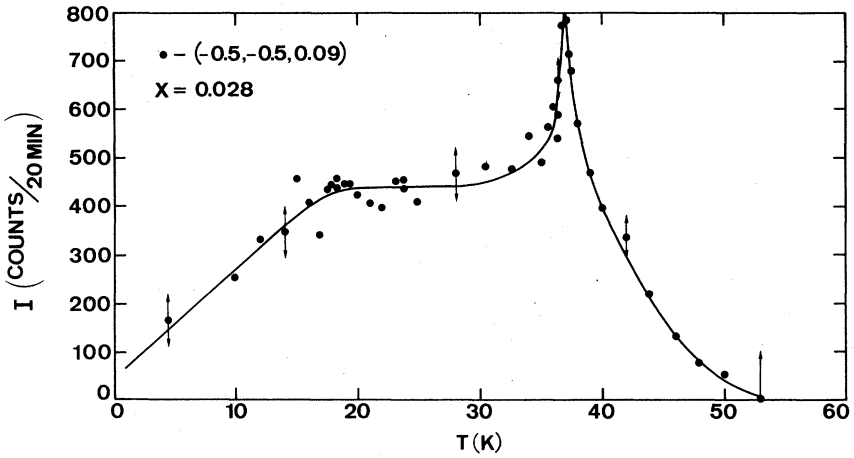

FIG. 14. Temperature dependence of the intensity of the ridge $[\frac{1}{2}\frac{1}{2}\zeta]$ for $x=0.028$ and for $\zeta=0.09$.

and 14, respectively. A striking feature in these plots is the appearance below T_c of a plateau of $d=2$ scattering. Such a phenomenon has hitherto not been observed in experiments on $d=2$ magnetic systems, in which the ridge intensity was always found to decrease continuously below T_c.[8,10,11] For the other two investigated samples this usual behavior was observed indeed, as is exemplified by Figs. 15 and 16, showing data for $x=0.061$ and $x=0.125$, respectively.

It is important to realize that the plateaus in the ridge intensities for the $x=0.022$ and $x=0.028$ samples cannot be due to critical scattering. As a function of temperature, the half width at half maximum (HWHM) of the ridge intensity (in q space) decreases continuously as T_c is approached from above, and reaches very nearly the experimental resolution limit at T_c itself. For $4\text{ K} < T \leq T_c$ the HWHM remains constant (within an accuracy of 30%), at a value of 0.007 Å^{-1}, corresponding with an intraplanar correlation length of about 150 Å. These values were obtained with aid of a deconvolution, taking into account $d=3$ resolution effects.[34] The fact that for $T_R < T < T_c - \Delta$ ($\Delta \simeq 4$ K) the ridge intensities observed for $x=0.022$ and 0.028 are independent of temperature indicates that this intensity is not due to $d=2$ LRO only, since in that case it would increase with decreasing temperature. The constant intensity may be explained by taking into account the additional contribution to the ridge intensity due to spin-wave scattering, which will probably increase linearly with temperature up to $0.9\ T_c$.[3] As seen in Figs. 15 and 16 we do find such a behavior for the $x=0.061$ and $x=0.125$ samples (which do *not* have $d=2$ LRO). For the $x=0.022$ and 0.028 samples in the region $T_R < T < T_c - \Delta$ the increase of the spin-wave contribution for increasing T is apparently compensated by the decrease of the contribution from $d=2$ LRO.

It should be noted that in the present study we are not able to distinguish between the contributions from $d=2$ spin-wave scattering and $d=2$ LRO on basis of a difference between their widths across the ridge, as has been done in Ref. 3 for

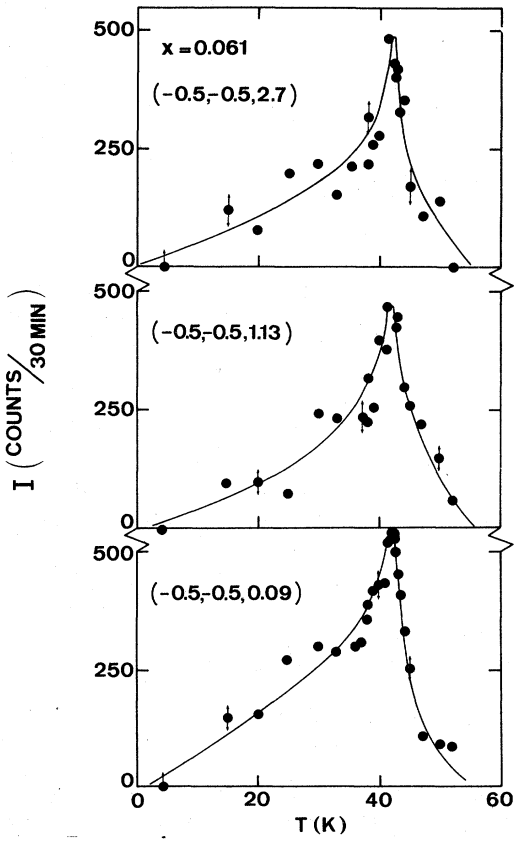

FIG. 15. Temperature dependences of the intensity of the ridge $[\frac{1}{2}\frac{1}{2}\zeta]$ for $x=0.061$ and for $\zeta=0.09$, 1.13, and 2.7.

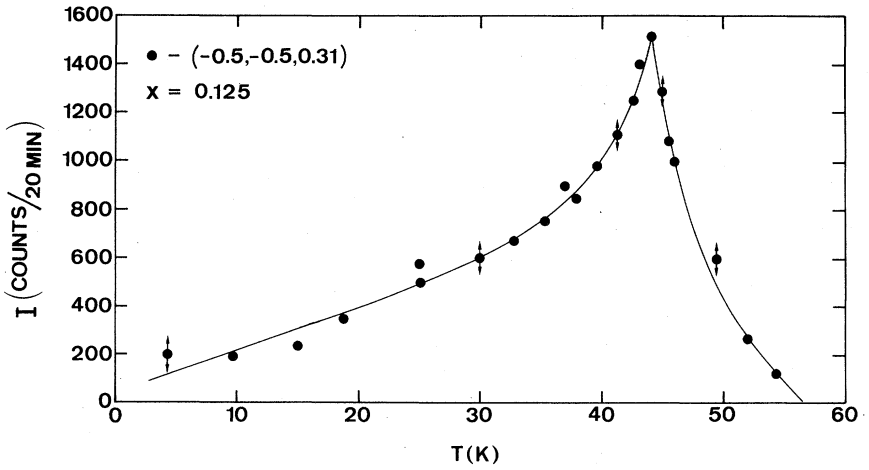

FIG. 16. Temperature dependence of the intensity of the ridge $[\frac{1}{2}\frac{1}{2}\zeta]$ for $x=0.125$ and for $\zeta=0.31$.

$Rb_2Mn_{0.5}Ni_{0.5}F_4$, because both widths are much smaller than the experimental resolution. However, the variation of the ridge intensity in the $x=0.022$ sample as a function of applied magnetic field H indicates that both contributions may be separated by performing a field cycle at constant temperature[35,36] (Sec. V B). The ridge intensity decreases in an irreversible way when the system is brought into the "spin-flop" phase, and the difference in $d=2$ intensity at $H=0$ before and after the cycle to $H=50$ kOe, observed at $T=15$, 27, and 33 K, scales qualitatively with the sublattice magnetization. On the other hand, the remaining ridge intensity after the field cycle increases with temperature.

The variation of the ridge intensities during a field cycle is hard to understand in terms of spin-wave scattering, since this would require rather unrealistic changes in the spin-wave gap during the field cycle (e.g., a change of the order of 20 K, whereas for pure K_2MnF_4 the gap is only 7.5 K). A more likely explanation is that the change in the ridge intensity corresponds to $d=2$ Bragg scattering, whereas the remaining part is due to spin-wave scattering. The same unrealistically large change in the gap energy would be needed to explain the effects seen at T_R in the present zero-field study.

It can be seen from Figs. 13 and 14 that the plateaus stretch from $T<T_c-\Delta$ to a temperature that corresponds in both cases with the reorientation temperature T_R. Below T_R the $d=2$ Bragg scattering gradually decreases, which matches the above-mentioned increase in the $d=3$ LRO for $T<T_R$ (see Sec. IV A). The values for $T_c(x)$ as defined by the peaks observed in the $d=2$ critical scattering are the same as found above from the $d=3$ Bragg reflections. From the variation of the $d=2$ scattering with the position at the ridge, we may further conclude the following. For $x=0.022$ the critical scattering at T_c originates mainly from the correlations between the z components of the spins, whereas the plateau intensities are mainly due to the $\langle S_xS_x\rangle$ and $\langle S_yS_y\rangle$ correlations. For $x=0.028$, on the other hand, both the critical scattering as well as the ridge intensity for $T_R<T<T_c-\Delta$ appear to involve more or less equally the z and xy components, although there is a tendency for the plateau intensity to contain more of the z components. The calculated and experimental normalized $d=2$ intensities are given in Table III.

As regards the reproducibility of the data in Figs. 13–16, we remark that the results shown were measured in a number of runs with different starting conditions and with both decreasing and increasing temperature. Within the experimental errors we could find no systematic differences between these runs. Therefore we conclude that the transfer of $d=2$ into $d=3$ order and vice versa appears to be a reproducible process.

We note that in his study on Rb_2CoF_4 Samuelsen[11] also mentions to have observed some remnants of the ridge intensity below T_c, remaining essentially unaltered in the investigated range below $0.9T_c$. Furthermore, he reports the width of the Bragg peaks and the intensity of the ridge to be strongly dependent on the rate of cooling through the transition. We have not found indications for such effects in the present experiments.

To investigate the behavior of the spin-wave scattering in the critical region we show in Fig. 17 the temperature dependence of the $d=2$ ridge intensity for the $x=0.061$ sample, plotted as $I_{max}-I$ vs $1-T/T_c$, where $I_{max}=I(T=T_c)$. This temperature dependence of $I_{max}-I$ corresponds

TABLE III. Measured and calculated intensities of the ridge $[\frac{1}{2}\frac{1}{2}\zeta]$ for several values of ζ, normalized with respect to the smallest ζ taken, for $T_R < T < T_c - \Delta$ ($\Delta \simeq 4$ K).

			Calculated	
	$x=0.022$	$x=0.028$	xy comp.	z comp.
$\frac{I(0.36)}{I(0.09)}$		1.00 ± 0.08	1.00	0.98
$\frac{I(0.72)}{I(0.09)}$		0.86 ± 0.07	1.05	0.72
$\frac{I(2.7)}{I(0.09)}$		0.58 ± 0.06	0.84	0.22
$\frac{I(0.72)}{I(0.36)}$	0.90 ± 0.08		1.02	0.82
$\frac{I(2.7)}{I(0.36)}$	0.74 ± 0.08		0.84	0.22

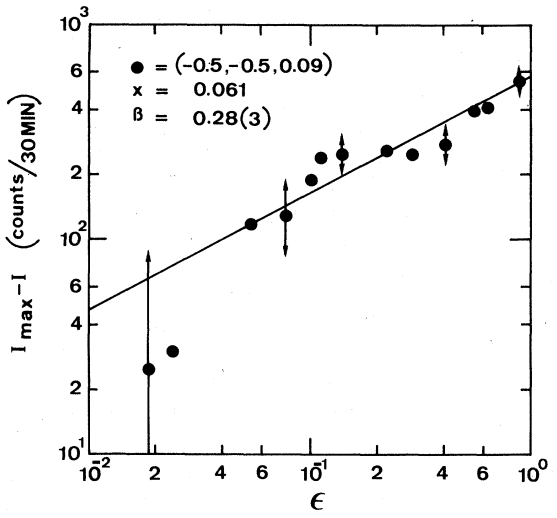

FIG. 17. Ridge intensity subtracted from the ridge intensity at T_c vs $\epsilon \equiv 1 - T/T_c$.

nicely with that observed in Fig. 11 for the Bragg peak ($\beta \simeq 0.28$ in both cases). Similar results are found for the $x=0.125$ sample. This indicates that the decrease in the ridge intensity below T_c is indeed complementary to the increase of the Bragg-peak intensity. The above results also indicate that the major part of the spin-wave scattering is concentrated on the ridge. This is indeed to be expected for quasi $d=2$ systems with a weak spin anisotropy.[3]

From the profiles of the ridge intensity close to T_c one may in principle also derive the critical behavior of the staggered susceptibility and of the correlation length. However, the present data are not sufficiently detailed or accurate to yield reliable information on these subjects.

V. DISCUSSION

A. Résumé

Some important conclusions to be drawn from the present experiments are the following. It appears that even in these doped materials a number of macroscopic quantities such as the net anisotropy, average sublattice magnetization, etc. are still well defined. In particular, it is surprising that the transitions to $d=3$ LRO at T_c appear to be as sharp as in the pure materials, such that one may even study the behavior of M_s in a substantial part of the critical region ($\epsilon \gtrsim 4\times10^{-3}$).

As expected the net anisotropy is a very sensitive function of the amount of Fe^{2+} or Co^{2+} impurities. Doping with Co^{2+} increases the net axial anisotropy, doping with Fe^{2+} lowers the net axial anisotropy until at a certain concentration between $x=0.022$ and 0.028 some "minimum" value is reached. At this "critical" concentration the net anisotropy changes from axial into planar. Subsequent increase of x brings about an increase in the net planar anisotropy.

The net anisotropy will be the result of the crystal-field anisotropy of Fe^{2+} or Co^{2+}, which will be nearly temperature independent, and the dipolar anisotropy that will vary with some power of the average sublattice magnetization. Thus the "average" anisotropy will be also dependent on temperature, which is clearly reflected in the observation of the reorientation phenomenon for the $x=0.022$ and $x=0.028$ samples.

B. $d=2$ and $d=3$ LRO for $x=0.022$ and $x=0.028$

An interesting outcome of the present study is the interlayer mismatching effects observed for the $x=0.022$ and $x=0.028$ samples. For these concentrations we are near the "anisotropy turning point," so that the directions of the spins will be quite inhomogeneously distributed throughout the lattice. As a consequence a minority of the spins is not involved in the $d=3$ LRO. This phenomenon seems to be quite analogous to the impurity effects observed in materials approximating linear magnetic chains.[1] For such substances the transition to $d=3$ LRO is brought about by the interchain interactions. It is found both experimentally and theoretically that the values of T_c for these systems are reduced dramatically upon introducing even a few percent of impurities. The process of randomly distributing impurity sites in an assembly of weakly coupled chains, will obviously result in a similar mismatch effect in the directions perpendicular to the chains.

With reference to the $x-T$ phase diagram given

in Fig. 9 we may explain our findings as follows. For the $x=0.022$ sample the $d=3$ ordering at T_c involves the z components of the spin system (cf. Table II). Between T_c and T_R one finds xy components that are only involved in $d=2$ ordering. These will be associated with those spins close enough to the Fe^{2+} impurities, to be nearly within the layers. Since the Fe^{2+} impurities are randomly distributed throughout each of the layers, a mismatching will occur between the spins inside such a $d=2$ cluster around the Fe^{2+} impurity and those Mn^{2+} spins that are in the adjacent layers. This explains why the lack of $d=3$ order involves the xy components. In lowering the temperature, the dipolar anisotropy will increase, so the net axial anisotropy will become larger, and the Mn^{2+} spins in the outer parts of the cluster will be pulled more and more out of the plane. At T_R and below reorientations take place, in which the $d=3$ ordered spins as well as the $d=2$ ordered spins gradually turn to a common (average) orientation that makes an angle of 35° with the c axis at $T=4.4$ K. The mismatching effect thereby becomes gradually more ineffective so that $d=2$ order is transferred into $d=3$ LRO. For the $x=0.028$ sample, a similar sequence of events occurs. Because of the higher Fe^{2+} content in this case the $d=3$ ordering below T_c entails the xy components, as can be seen from both the χ data and the neutron scattering results. Since apparently the major part of the spins are now within the layers, the mismatching effect will include the z components of the spin system, in agreement with observations (cf. Fig. 9 and Table III). As the spins within the layers may point in either the [110] or the $[\bar{1}10]$ direction there will also be some mismatching in the correlations in x and y directions, both within the same plane and in adjacent layers. This explains why for the $x=0.028$ sample the ridge intensity contains xy as well as z components. In lowering the temperature the net planar anisotropy will decrease because of the growing importance of the axial dipolar anisotropy. The system again finds a compromise below T_R, which now brings about a rotation of the moments to a mean orientation at an angle of 60° with the c axis, i.e., closer to the layers than for $x=0.022$.

For both samples the reorientation phenomenon and the accompanying transfer of $d=2$ into $d=3$ LRO appear to be characterized by the absence of hysteresis in cycling the temperature.

Recently, we have extended our measurements by performing a field-dependent neutron-diffraction study[35,36] on the $x=0.022$ sample in magnetic fields up to $H=50$ kOe applied along [001]. The results may be briefly summarized as follows. The coexistence of $d=2$ and $d=3$ LRO between T_R and T_c is confirmed. This coexistence range on the T axis is found to become extended into a two-dimensional region in the H-T diagram. Furthermore, the transfer of $d=2$ into $d=3$ LRO can also be induced by increasing the field, which is applied parallel to the c axis, at constant temperature. Once the "spin-flop region" has been entered, this transfer becomes complete [at all temperatures below $T_c(H)$]. If the field is subsequently decreased the system remains fully $d=3$ ordered. Thus the reversibility is lost as soon as the spin-flop phase is reached. The H-dependent transfer process may be understood by considering that in approaching the spin-flop phase the moments that were initially parallel to the c axis (i.e., those involved in the $d=3$ LRO) will become oriented perpendicular to the c axis. Since the moments involved in the $d=2$ LRO were already oriented mainly perpendicular to the c axis, it follows that upon entering the spin-flop phase the mismatching effect will have been removed and the $d=3$ correlations can be fully established. Apparently the latter correlations are not destroyed when, upon decreasing the field again, the spins are rotating back into the direction of the c axis. The difference in reversibility between the two ways of transferring $d=2$ into $d=3$ LRO will be due to the fact that the spin-flop process is a cooperative (many-body) phenomenon, whereas the T-dependent transfer (for $H=0$) will be the result of local phenomena, namely, the local changes in the net spin anisotropy. A full discussion of these H-dependent neutron-diffraction data will be given in a forthcoming paper.[36]

The x-T phase diagram shown in Fig. 9 bears a strong resemblance to that recently published by Aharony and Fishman[37] for a randomly mixed two-component spin system with competing interaction anisotropies. They find two critical lines, each corresponding to the ordering of the spin components favored by one type of spin anisotropy. The two phase lines *cross* in a *tetracritical* point, so that the ordered region is divided into three parts, namely, one in which the z components are ordered, one in which the xy components are ordered, and an intermediate phase characterized by mixed ordering. The experimental observation of the two transitions (T_c and T_R) would thus be explained, as well as the fact that the ordering at T_c entails the z and xy components for the $x=0.022$ and 0.028 sample, respectively.

In spite of the nice correspondences between the Aharony-Fishman model[37] and our experimental results we would like to point out some of the complications introduced, e.g., by the quasi-two-dimensionality of the experimental compounds. This leads to uncertainties as regards the factors determining the value of T_c, as will be further

discussed below. Furthermore, the $d=2$ order observed for $T_R < T < T_c$ is of course not a direct consequence of the Aharony-Fishman (AF) model. Moreover, the AF model considers classical spins.

C. Critical behavior

Inspection of the values measured for the apparent critical exponent β, as compiled in Table I, shows that for the Fe-doped samples the value of β at first increases with x, passes through a maximum that coincides with the minimum in T_c, and thereafter decreases again to $\beta \simeq 0.21$ for $x=0.125$. This rather high value may be due to the limited part of the critical region covered in our experiments. For instance, in a recent study on the $d=2$ iron compound $(CH_3NH_3)_2FeCl_4$ Keller *et al.*[29] found $\beta=0.146$ from data in the range $2\times10^{-4} \leq \epsilon \leq 10^{-2}$, whereas previously they had deduced $\beta \simeq 0.21$ from measurements in the range $\epsilon > 2\times10^{-2}$. In spite of these uncertainties regarding the true critical behavior in our doped samples, it is clear, however, that the shape of the magnetization curves just below T_c is certainly strongly dependent on the type and the amount of impurity. It is noteworthy that the Co-doped sample appears to show the same value of β as the pure K_2MnF_4 compound. The reason could be that in both cases the anisotropy is axial. A similar result has recently been reported by Als-Nielsen *et al.*[2] in a study on the system $Rb_2Mn_{0.5}Ni_{0.5}F_4$. The pure Ni compound also has axial anisotropy. These authors likewise found a well-defined phase transition, with critical exponents for M_s, χ_{stagg}, and the correlation length identical to those of the pure Mn and Ni compounds.

The conclusion seems therefore that the variation in β must be due to the competing anisotropy mechanisms in case of the Fe-doped systems. We can offer the following explanation, although this has to be speculative because of our limited amount of data. The correlation between the β values and the amount of spin-anisotropy suggests that by decreasing the latter the nature of the phase transition has changed from one that is primarily anisotropy induced, into one that is also influenced by the $d=3$ interlayer interaction. This would explain why the highest β value observed is close to the $d=3$ Ising value of $\beta=0.31$. In pure K_2MnF_4 the dimensionality crossover from $d=2$ to $d=3$ Ising behavior of $M_s(T)$ apparently occurs closer to T_c than $\epsilon \simeq 2\times10^{-3}$.[8] The crossover point will be dependent on the ratio of the Ising spin anisotropy to the interlayer interactions, and would thus be shifted to higher ϵ values upon decreasing the former. Since it is noted that the planar anisotropy is ineffective in producing long-range order in $d=2$ lattices, the ordering in the Fe compounds has to be the result of the anisotropy within the easy plane of magnetization. In Fig. 18 we compare our results for $x=0.028$ (which has $\beta=0.28$) with published data for the $d=2$ systems K_2MnF_4, Rb_2FeF_4, and $(CH_3NH_3)_2FeCl_4$ as well as for the $d=3$ compound MnF_2. It is quite remarkable how much closer our results are to those of MnF_2 than to those of the $d=2$ systems. On the otherhand, the curve for the $K_2Mn_{0.98}Co_{0.02}F_4$ sample is quite near to that for the pure K_2MnF_4 (cf. Fig. 10).

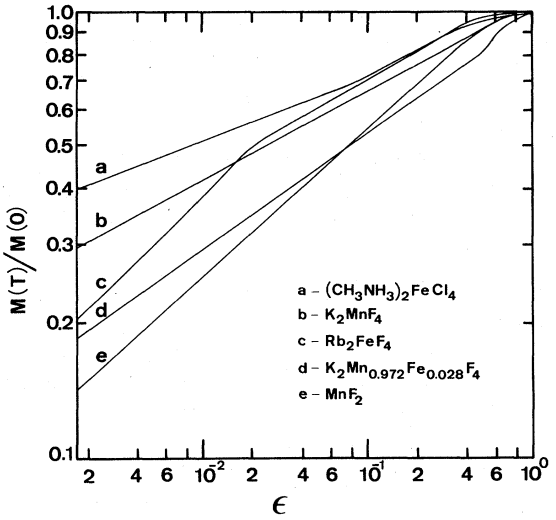

FIG. 18. Normalized sublattice magnetization $M(T)/M(0)$ vs ϵ for several compounds.

Another possible explanation for the large β values for $0.022 \leq x \leq 0.061$ could be that for these concentrations one is near to the tetracritical point defined by the intersection of the two critical lines in the x-T phase diagram, according to Aharony and Fishman. However, it is not clear yet whether the approach of the tetracritical point along these critical lines would indeed entail a change in the exponents.

ACKNOWLEDGMENTS

We thank Dr. D. J. Breed for the preparation of the single crystals. Dr. H. Kragten is acknowledged for the chemical analyses of the samples. We also thank Professor Dr. H. W. de Wijn and co-workers for sending us the tabulated data on K_2MnF_4 and K_2FeF_4. We are indebted to Dr. H. Keller *et al.* for sending his tabulated data on $(CH_3NH_3)_2FeCl_4$. Professor Dr. W. J. Huiskamp and Dr. J. Bergsma are thanked for correcting the manuscript and for their interest in the work. The technical assistance of H. H. A. Plas during the experiment was very valuable.

[1]See, e.g., Proc. ICM, 1976, Amsterdam, part II, Chap. 4 (Physica B 86–88, 1977).
[2]J. Als-Nielsen, R. J. Birgeneau, H. J. Guggenheim, and G. Shirane, J. Phys. C 9, L121 (1976).
[3]R. J. Birgeneau, J. Als-Nielsen, and G. Shirane, Phys. Rev. B 16, 280 (1977).
[4]R. J. Birgeneau, L. R. Walker, H. J. Guggenheim, J. Als-Nielsen, and G. Shirane, J. Phys. C 8, L328 (1975).
[5]R. A. Cowley, G. Shirane, R. J. Birgeneau, and H. J. Guggenheim, Phys. Rev. B 15, 4292 (1977).
[6]D. J. Breed, Physica 37, 35 (1967).
[7]D. J. Breed, thesis (University of Amsterdam, 1969) (unpublished).
[8]R. J. Birgeneau, H. J. Guggenheim, and G. Shirane, Phys. Rev. B 1, 2211 (1970).
[9]D. J. Breed, K. Gilijamse, and A. R. Miedema, Physica 45, 205 (1969).
[10]H. Ikeda and K. Hirakawa, Solid State Commun. 14, 529 (1974).
[11]E. J. Samuelsen, J. Phys. Chem. Solids 35, 785 (1974).
[12]H. Ikeda and K. Hirakawa, J. Phys. Soc. Jpn. 33, 393 (1972).
[13]G. K. Wertheim, H. J. Guggenheim, H. J. Levinstein, D. N. E. Buchanan, and R. C. Sherwood, Phys. Rev. 173, 614 (1968).
[14]M. P. H. Thurlings, A. van der Pol, and H. W. de Wijn, Solid State Commun. (to be published).
[15]L. J. de Jongh and A. R. Miedema, Adv. Phys. 23, 1 (1974).
[16]N. D. Mermin and H. Wagner, Phys. Rev. Lett. 17, 1133 (1966).
[17]L. Onsager, Phys. Rev. 65, 117 (1944).
[18]M. E. Lines, Phys. Rev. 164, 736 (1967).
[19]K. Binder and D. P. Landau, Phys. Rev. B 13, 1140 (1976).
[20]N. W. Dalton and D. W. Wood, Proc. Phys. Soc. 90, 459 (1967).
[21]T. Ishikawa and T. Oguchi, J. Phys. Soc. Jpn. 31, 1021 (1971).
[22]L. Bevaart, E. Frikkee, and L. J. de Jongh, *Proceedings of the Conference on Neutron Scattering, Gatlinburg, 1976.* edited by R. M. Moon (National Technical Information Service, U.S. Department of Commerce, Springfield, Virginia 22161), p. 697.
[23]L. Bevaart, J. V. Lebesque, E. Frikkee, and L. J. de Jongh, Physica B 86–88, 729 (1977).
[24]L. Bevaart, E. Frikkee, J. V. Lebesque, and L. J. de Jongh, Solid State Commun. 25, 539 (1978).
[25]R. de Pape, Bull. Soc. Chim. France 3489 (1965).
[26]Y. Tamminga, thesis (Amsterdam, 1973) (unpublished).
[27]L. W. Roeland, F. A. Muller, and R. Gersdorf, Coll. Int. Cent. Natl. Rech. Sci. 166, 175 (1967).
[28]H. W. de Wijn, R. E. Walstedt, L. R. Walker, and H. J. Guggenheim, Phys. Rev. B 8, 285 (1973).
[29]H. Keller, W. Kündig, and H. Arend, Proceedings of the Mössbauer Conference, Korfu, Greece, 1976 (unpublished).
[30]J. V. Lebesque, J. H. P. Colpa, and L. Bevaart, Physica B (to be published).
[31]M. E. Fisher, Rev. Mod. Phys. 46, 597 (1974), and references therein.
[32]L. J. de Jongh and H. E. Stanley, Phys. Rev. Lett. 36, 817 (1976).
[33]R. J. Birgeneau, J. Skalyo Jr., and G. Shirane, J. Appl. Phys. 41, 1303 (1970).
[34]A. L. M. Bongaarts, RCN Report No. RCN-235, 1975 (unpublished).
[35]L. Bevaart, E. Frikkee, and L. J. de Jongh, Proceedings of the Conference STATPHYS 13, Haifa, 1977, Ann. Israel Phys. Soc. and to be published.
[36]L. Bevaart, E. Frikkee, and L. J. de Jongh, Solid State Commun. 25, 1031 (1978), (to be published).
[37]A. Aharony and S. Fishman, Phys. Rev. Lett. 37, 1587 (1976).